Topography and work function measurements of thin MgO(001) films on Ag(001) by nc-AFM and KPFM

M. Bieletzki,[a] T. Hynninen,[bc] T. M. Soini,[a] M. Pivetta,[d] C. R. Henry,[e] A. S. Foster,[bc] F. Esch,[a] C. Barth*[e] and U. Heiz[a]

Received 9th November 2009, Accepted 12th January 2010
First published as an Advance Article on the web 11th February 2010
DOI: 10.1039/b923296f

The surface topography and local surface work function of ultrathin MgO(001) films on Ag(001) have been studied by noncontact atomic force microscopy (nc-AFM) and Kelvin probe force microscopy (KPFM). First principles calculations have been used to explain the contrast formation of nc-AFM images. In agreement with literature, thin MgO films grow in islands with a quasi rectangular shape. Contrary to alkali halide films supported on metal surfaces, where the island heights can be correctly measured, small MgO islands are either imaged as depressions or elevations depending on the electrostatic potential of the tip apex. Correct island heights therefore cannot be given without knowing the precise contrast formation discussed in this paper. KPFM shows a silver work function which is reduced by the MgO islands. The values for the work function differences for one and two layer thin films are −1.1 and −1.4 eV, respectively, in good agreement with recent calculations and experiments.

In recent years magnesium oxide has become the focus of intensive research due to its important role as an interface material in many applications, for example, as a magnetic tunnel junction or as a high-*k* dielectric in electronic devices,[1,2] and particularly as a support material in catalysis.[3–7] The MgO (001) interface has become one of the major model surfaces[8–10] for the study of charge, size, morphology and nucleation control of supported clusters, and hence a corner stone of 'nanocatalysis' research.[11,12]

As far as these interface properties for the catalysis of supported clusters are concerned, the cluster/oxide system as a whole has been noted as playing a key role.[12] In particular, if the oxide is ultrathin MgO(001) grown on metal substrates, the work function of the MgO(001)/metal system is substantially lowered[13–16] and deposited gold clusters, for instance, become charged.[8,9] Thus the underlying metal substrate changes the geometry and electronic properties of the supported cluster/oxide system, as long as the oxide films are thinner than about four monolayers.[17] These effects pave the way for tuning the cluster/oxide systems in catalytic applications by interface engineering. Indeed, recently it has been illustrated that the reduction of the work function and the concomitant charging and structural changes influence the catalysis of supported gold clusters on MgO(001) thin films.[5] A prerequisite of tuning cluster/oxide systems in catalysis is, hence, a precise knowledge of the local work function of oxide thin films and its dependence on the surface structure and morphology at the nanometre scale.

In recent years, scanning tunneling microscopy (STM) has successfully shown that the surface structure and morphology of thin MgO films on various metal substrate surfaces can be imaged with the highest precision.[18–23] So far, work function measurements of thin MgO films have been done with integral analysis methods, like ultraviolet photoelectron spectroscopy, metastable impact electron spectroscopy,[24,25] two-photon photoemission spectroscopy (2PPS)[26] or Auger electron spectroscopy.[27] However, a simultaneous analysis of the surface structure/morphology and of the surface work function at the nanometre scale is still missing, but highly desirable.

Frequency-modulated noncontact atomic force microscopy (nc-AFM)[28–30] has been shown recently to be as equally capable as STM to image oxide surfaces,[31] even with atomic resolution.[32] An advantage of nc-AFM is the implementation of the Kelvin modulation technique.[33] This so-called Kelvin probe force microscope (KPFM) provides an image of the local work function of the surface in parallel to the acquisition of the topography image. For instance, the KPFM could successfully be applied for work function measurements of palladium clusters supported on bulk MgO(001).[34] First measurements of thin alkali halide films on metal surfaces have shown that thin films can also be well characterized with a lateral resolution of several tens of nanometres and with a voltage resolution in the mV range.[35,36] The lateral resolution is given by the size of the tip apex, which has been quantitatively explained by recent measurements.[37] Although MgO(001) thin films were imaged with atomic resolution[38] and some primarily electrostatic force spectroscopy (EFS) measurements have been done,[39] no work can be found to date that deals with a complete nc-AFM and Kelvin microscopy investigation of MgO(001)/Ag(001) thin films at the nanometre scale.

[a] *Lehrstuhl für Physikalische Chemie, Technische Universität München, Department Chemie, Lichtenbergstr. 4, D-85748 Garching, Germany*
[b] *Department of Physics, Tampere University of Technology, P.O. Box 692, FIN-33101 Tampere, Finland*
[c] *Laboratory of Physics, Helsinki University of Technology, P.O. Box 1100, 02015, Finland*
[d] *Ecole Polytechnique Fédérale de Lausanne, Institut de Physique de la Matière Condensée, CH-1015 Lausanne, Switzerland*
[e] *Centre Interdisciplinaire de Nanoscience de Marseille (CINaM, The CINaM is associated with the Universities of Aix-Marseille II and III), CNRS, Campus de Luminy, Case 913, 13288 Marseille Cedex 09, France. E-mail: barth@cinam.univ-mrs.fr*

In this paper, thin MgO(001) films supported on Ag(001) surfaces are explored by nc-AFM and KPFM measurements. Two types of quasi rectangular islands could be found where one type of islands is supported on the silver surface and the second type is embedded in the substrate surface. Mainly three types of topography contrasts exist, depending on the polarity of the tip, in fundamental contrast to the imaging of alkali halide films grown on metal surfaces.[35–37,40] Kelvin images represent the MgO islands with dark contrast, which corresponds to a lower work function with respect to the silver substrate. One and two layer high islands lower the silver work function by $\Delta\phi_{1\text{-layer}} = (-1.1 \pm 0.2)$ eV and $\Delta\phi_{2\text{-layer}} = (-1.4 \pm 0.2)$ eV, respectively, in good agreement with the values expected from theory.[13,14,41]

1. Experiment and theory

Frequency-modulated nc-AFM and KPFM experiments were performed in the low 10^{-10} mbar pressure range and at room temperature with an VT Omicron AFM/STM. A conducting silicon cantilever (Nanosensors, p-Si, 0.015 Ω cm, 318 kHz resonance frequency, 29 N m^{-1} spring constant, 10 nm peak-to-peak amplitude) was used. Since the tip was originally exposed to the atmosphere, it carried a native oxide layer before taking measurements.

In frequency-modulated KPFM,[33,42] a dc (U_{dc}) and ac voltage (U_{ac}) with frequency f_{ac} are applied between the tip and surface.[43] In a KPFM measurement, the electrostatic tip–surface interaction is minimized at each point on the surface by the dc voltage, which yields the contact potential difference between tip and surface $U_{dc} = (\phi_{sample} - \phi_{tip})/e$. If the contact potential difference is measured at two different locations on the surface (position 1 and 2), the difference $(U_{dc,pos1} - U_{dc,pos2})*e = (\phi_{pos1} - \phi_{tip}) - (\phi_{pos2} - \phi_{tip}) = \phi_{pos1} - \phi_{pos2} = \Delta\phi$ yields the work function difference between the two surface locations.[33] If fixed charges are present on the surface, they change the work function depending on their strength and sign.[44,45] The Kelvin modulation is applied during normal topography imaging, so that both, a topography and a Kelvin image, are obtained in one measurement. All images were acquired in the constant detuning mode with the Omicron Matrix system and prepared with the Gwyddion[46] software.

The silver surface of a single crystal (Surface Preparation Lab, Holland, 99.999%, surface polished with 0.1° degree precision) was prepared by several cycles of ion sputtering (1.0 keV, 40 min) and annealing (550 °C, 30 min) followed by slow cooling (10 K min^{-1}) for optimizing terrace widths. A thin MgO(001) film was then grown by evaporating Mg from a hot magnesium ribbon band ($\sim$0.1 ML min^{-1}) in an oxygen atmosphere (1×10^{-6} mbar). The sample temperature was kept at 215 °C and then slowly cooled down to room temperature after the preparation. All preparation steps and AFM measurements were done in the same UHV chamber.

The calculations have been performed using the periodic plane-wave basis VASP[47,48] code, implementing the spin-polarized density functional theory (DFT) and the generalized gradient approximation.[49] Projected augmented wave (PAW) potentials[50,51] were used to describe the core electrons. The potential for O was generated in the electron configuration $[1s^2]2s^22p^4$, Mg in $[Ne]3s^2$ and Ag in $[Kr]4d^{10}5s^1$, with the core electrons given in square brackets. A kinetic energy cutoff of 400 eV and a $2 \times 2 \times 1$ k -point Monkhorst–Pack grid[52] was found to converge the total energy of the systems to within 10 meV. This setup reproduced the experimental bulk structural properties of MgO and Ag to within 2%. Calculations were also corrected for artificial electrostatic interactions in the periodic system, if present, by calculating monopole and dipole corrections explicitly. To model the surface of Ag and MgO thin films, slabs with their (001) surfaces exposed, separated by a sufficient vacuum gap (always at least 1 nm) were set up. For Ag, a slab of four atomic layers with the two lowermost layers frozen was found to be thick enough to mimic the surface of a semi-infinite bulk. Similarly, MgO thin films were described by four layers of Ag and one layer of MgO supported on top of the Ag surface with the two lowermost layers frozen. Upon introducing the MgO layer, the calculations gave a lowering of the silver work function of about 0.96 eV, in good agreement with previous calculations.[13,14,41] Note that this value did not change significantly when either metal, neutral or charged tips where added to the system, indicating that artificial charge transfer from the surface to the tip is not present.

It is well-known that tips in nc-AFM, despite being originally silicon, are contaminated by the ambient and contact with the surface, hence their structure and chemistry is unknown on the nanoscale. In order to represent this, a variety of tip models including stoichiometric and non-stoichiometric MgO, and Ag clusters are considered. The Ag tip is modeled as a 20 atom cluster in the shape of a tetrahedron with one of the vertices pointing towards the surface. The stoichiometric MgO tips are $Mg_{32}O_{32}$ cubes, with both Mg and O terminated tips represented by turning the corresponding vertex towards the surface. The non-stoichiometric MgO tips are constructed from the stoichiometric ones by removing atoms at the cube vertex furthest from the surface, resulting in $Mg_{29}O_{31}$ and $Mg_{31}O_{29}$ structures. Although these tips are also terminated either by a single Mg^{2+} or O^{2-} being closest to the surface as in the case of the stoichiometric MgO tips, the different amount of Mg and O atoms at the cube vertex furthest from the surface results in the tips being electrostatically more polarized than their stoichiometric counterparts. The resulting dipole moment of 8 Debye for both polar tips is relatively large in comparison to the one of the stoichiometric tips (1 Debye), but comparable with the dipole of a MgO molecule for instance (6.2 Debye[53]). The latter MgO molecule is just one possible candidate amongst a variety of possible polar tips and can be strongly adsorbed at a MgO cluster at the tip for instance.[54] In the following, a tip terminated with an Mg^{2+} ion and an excess of oxygen at the cube vertex furthest from the surface is called *positive polar tip*, and, *vice-versa*, a tip terminated by an O^{2-} ion with an excess of magnesium at the cube vertex furthest from the surface is called *negative polar tip*.

The forces experienced by the model tips are explicitly calculated for heights of 2 to 6 Å above the surfaces. For tip–surface distances of more than 6 Å, the forces are extrapolated. In order to compare directly to experimental frequency changes, the calculated tip–surface forces were used as input for a model of cantilever dynamics using experimental

parameters.[30] Only at tip approaches of less than 5 Å were small tip-induced surface atom displacements observed, which increased the calculated forces.

2. Results and discussion

2.1 Topography imaging

The topography images in Fig. 1 show characteristic details, which appear during nc-AFM imaging of thin MgO(001) islands of roughly 0.3 ML on Ag(001). In Fig. 1a, two atomically flat silver terraces can be seen, separated by a one-layer-high step. On the silver terraces, the thin MgO(001) film is composed by small islands with a mean size of 6×6 nm^2, which is in agreement with previous findings.[55] The islands have an almost rectangular shape and appear with a density of 6.6×10^{11} islands cm^{-2} on the silver surface, similar to previous studies.[21] Clearly visible is a strongly pronounced contrast at the edges of the films, which is composed of dark and bright dots. As previously observed by STM,[23] the dots might be defects such as F centers at low coordinated sites at the edges of the islands or trapped electrons at Mg corners.[62]

The most striking observation, however, is that the islands were imaged as depressions, as can be seen in the profile below Fig. 1a. Two types of island depth exist—one type of island is imaged with an apparent depth of $\Delta z_{\mathrm{MgO-a}} = -3.1$ Å whereas a few islands were imaged with a depth of $\Delta z_{\mathrm{MgO-b}} = -1.2$ Å. In the following, the two types of islands are called $\mathrm{MgO_a}$ and $\mathrm{MgO_b}$ islands, respectively. These observations suggest that most of the MgO islands are almost −3 Å below the silver surface, which is in strong contradiction to previously published STM measurements[18–20,22] and to our STM measurements obtained on the same samples (results not shown here) that show the presence of embedded and supported islands at high biases ($U_{\mathrm{bias}} \geqq 3$ V).

In order to understand better the contrast formation of this system, image b of Fig. 1 was obtained directly after image a without any change of the scanning parameters. In the first, lower part of the image (scanning was performed from the bottom to the top), the same contrast can be found as in image a. After two thirds of the image, a tip-change leads to a completely different appearance of the MgO islands. The $\mathrm{MgO_b}$ islands appear now as bright elevations with a height of $\Delta z_{\mathrm{MgO-b}} = +1.7$ Å, whereas the $\mathrm{MgO_a}$ islands seem to be still below the surface ($\Delta z_{\mathrm{MgO-a}} = -0.4$ Å). After a second tip-change, the contrast changed again drastically. Both islands appear now as bright islands with height differences of $\Delta z_{\mathrm{MgO-b}} = +2.2$ Å and $\Delta z_{\mathrm{MgO-a}} = +0.3$ Å with respect to the silver surface. For a more detailed representation of the tip-induced contrast change at the MgO islands, a representative island is shown in image c and d with a higher magnification. In a further image (e), a contrast similar to the one after tip-change I was found above the same islands ($\Delta z_{\mathrm{MgO-a}} = -0.6$ Å and $\Delta z_{\mathrm{MgO-b}} = +1.2$ Å). Note that the difference in apparent height between both types of MgO islands ($\Delta z_{\mathrm{MgO-b}} - \Delta z_{\mathrm{MgO-a}}$) is very close to the silver step height of $\sim$2.0 Å.[41,56]

Tip-induced changes of the contrast are a well-known phenomenon in nc-AFM of ionic tip–surface systems and occur at distances of typical chemical bond lengths,[30] as has been shown on the (111) surface of CaF_2.[57] Generally, before obtaining high resolution images as shown in Fig. 1, several tip-changes occur and it can be strongly anticipated that the tip picks up Ag atoms or magnesium or oxygen ions. The tip can therefore carry silver atoms, an anion (O^{2-}) or cation (Mg^{2+}) or a more complex charged system where the local stoichiometry of MgO is disturbed such that the tip presents a strong dipole. Note that the tips used here were not additionally prepared after their transfer into the UHV chamber and thus carry a native silicon oxide layer, which prevents discharging of ionic material at the tip on the time-scale of the image acquisition.[58]

If the electrostatic potential of the tip influences the contrast of MgO(001) islands on the silver surface, the change of contrast can be qualitatively explained as follows: If it is assumed that a polar tip is positioned at a typical distance of 5–20 Å above the silver surface (Fig. 2a, left), the electrostatic polarization of the silver surface by, *e.g.*, a negative tip is sufficiently strong to produce a measurable electrostatic dipole force. The electrostatic force is attractive, and this does not change if the same dipole at the tip is flipped (Fig. 2a, right). This can be the case if, for example, a MgO tip carrying an excess of oxygen is replaced by a MgO tip with the same excess of magnesium. As both electrostatic interactions exhibit the same strength, no change in the topography signal should be visible during such a tip change above the silver surface.

A MgO interface in between the surface and the tip, however, breaks this symmetry: as shown recently, one-layer-thin MgO(001) films supported on silver (001) lower significantly the work function of the silver surface, mainly due to a charge transfer between the film and the support.[13,14,41] Calculations show that the charge transfer is relatively large for one layer thin MgO films (1.35×10^{-2} electrons Å^{-2}) in comparison to other films like NaCl of same thickness (0.22×10^{-2} electrons Å^{-2}).[41] This leads to a dipole perpendicular to the surface, with the MgO(001) surface carrying a positive net surface charge. If the tip has a dipole in opposite direction (positive polar tip) there will be repulsive forces between the tip and the positive MgO island. The opposite scenario appears, if the dipole of the tip is flipped (negative polar tip)—the resulting force is attractive.

In order to check whether the electrostatic forces are indeed sufficiently large to explain the latter model, first principles simulations of the experiments shown in Fig. 1 have been performed. Here the tip–surface force was directly calculated for several tips over the Ag surface and a monolayer MgO thin film—note that the simulated systems are separated, so both, the Ag surface and the MgO film were at the same effective height. As shown in Fig. 3, there is no significant difference in calculated frequency changes on the Ag surface and one layer MgO thin films for silver tips and stoichiometric MgO tips, which are designated as *neutral tips* in the following. This means, for example, that if a one-monolayer-thin MgO island is supported on the Ag surface, the expected step height of $\sim$2.5 Å[41,56] should be roughly well represented in a topography image. The change in apex atom certainly changes the nature of the local electrostatic potential, but this would only influence contrast in atomically resolved images.[30,59]

The large tip-dependent contrast changes seen in experimental images can only be understood if the difference in

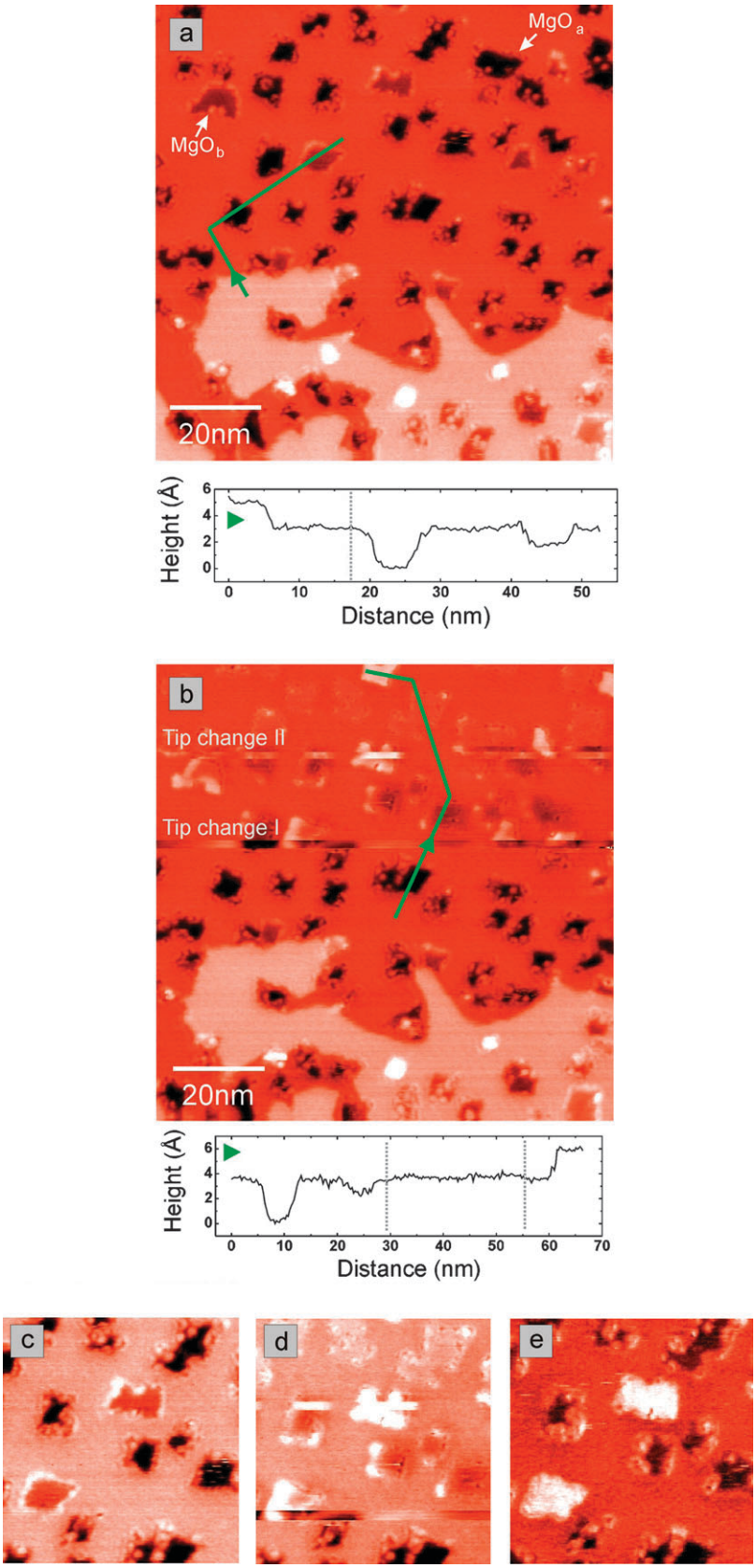

Fig. 1 (a,b) Topography images of two consecutive measurements representing a typical contrast of small MgO(001) islands on the Ag(001) surface. The scanning parameters were not changed between the measurements. 100 × 100 nm^2, $\Delta f = -30$ Hz, $v_{Scan} = 0.5$ Hz, $U_{ac} = 0.3$ V, $f_{ac} = 630$ Hz. (c–e) Details of the same sequence.

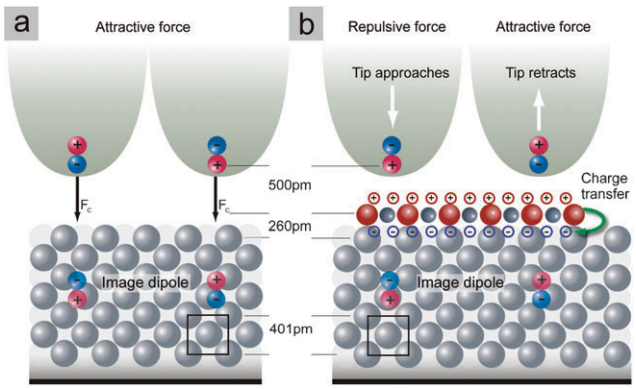

Fig. 2 The tip with positive or negative dipole above the silver surface (a) and above an one layer thin MgO(001) island (b). The ion–ion distances in MgO and atom–atom distances in silver are true to scale.

forces between different non-stoichiometric MgO tips—*negative and positive polar tips*—are considered. Here the dipole–dipole interaction introduces much longer ranged interactions. For the reduced MgO tip and a dipole pointing in the same direction as the thin film dipole (negative polar tip), a long-range attractive force is obtained. For a positive polar MgO tip, the dipole points in the opposite direction and a long-range repulsive force is obtained. The absolute magnitude of the simulated frequency changes is plotted in Fig. 3 and is a direct function of the strength of the long-range forces, and hence characteristic of that particular tip. As such it should be possible to reproduce quantitatively all the measured contrast changes in experiments by varying the structure of tip. When contacting the surface, the probability of creating a polar tip should be of the same order as that of a neutral tip, as it is unlikely that only stoichiometric material will be transferred. However, fully stoichiometric tips are certainly more stable with respect to further tip changes.

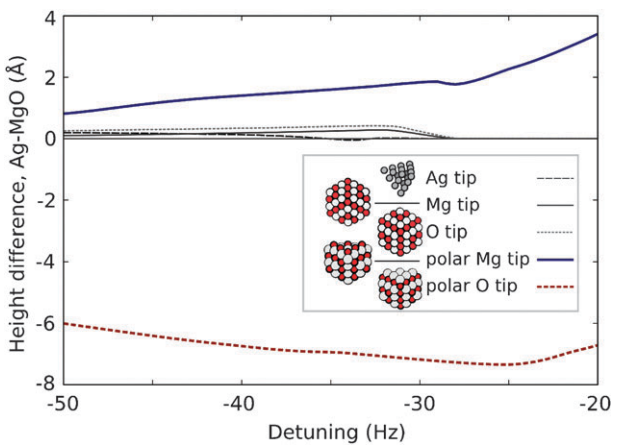

Fig. 3 The difference in apparent heights between the Ag bulk and MgO thin film surfaces for different tip models as a function of detuning Δf (white and red circles represent magnesium and oxygen ions, respectively). The apparent height is the height seen by the nc-AFM with respect to the true surface level. A positive height difference means that for Ag and MgO surfaces at the same height level, Ag is imaged higher. *Vice-versa*, a negative value means that MgO appears as higher. For a stepped surface, the difference in imaged heights would be the step height plus the difference in apparent height. Detuning values of −50, −30 and −20 Hz correspond to tip–surface distances of about 3, 5 and 10 Å.

Therefore, neutral tips carrying silver atoms or neutral ionic MgO compounds reproduce embedded or supported MgO islands with almost the correct height values in topography images. However, strongly polar tips falsely reproduce the height values of MgO islands. In the extreme, *e.g.* for tips strongly polarized in opposite direction to the thin film polarization (positive polar tips), the islands are imaged as depressions. In this case, when the tip passes from the silver surface to the MgO island, the force gets more repulsive (less attractive) and a smaller detuning Δf results. The distance regulation loop approaches the tip to the surface, until the attractive van der Waals contribution outbalances the repulsion and the initial detuning Δf is recovered—the MgO islands appear as depressions in the images. The same imaging mechanism happens for tips strongly polarized in the same direction as the thin film polarization (negative polar tips), but with opposite behavior: the tip is retracted in order to reduce the force that became more attractive over MgO. Consequently the MgO islands appear in a brighter contrast, overestimating their height.

Similar to what can be observed in STM images with elevated, positive bias voltages ($U_{bias} \geqq 3$ V), the MgO_a and MgO_b islands in Fig. 1 are attributed to partially embedded and supported islands, respectively, each one layer thick as expected for these coverages.[18,19,56] The MgO islands visible in image a and b (until tip-change II) of Fig. 1 were imaged with a polar tip, the dipole of which was antiparallel to the one of the MgO islands (positive polar tip). It is obvious that after tip-change II, the tip changed to a neutral tip because the two types of MgO islands were indeed imaged as embedded and supported islands, as expected.[18,19,56] The height difference between both types of islands ($\Delta z_{MgO-b} - \Delta z_{MgO-a} = 2.0$ Å) equals almost the step height of silver, which means that the embedded islands are supported on the second silver layer below the top surface layer.[56] Merely the height of the supported MgO_b islands of $\Delta z_{MgO-b} = 2.2$ Å with respect to the silver terraces is a little bit smaller than predicted by theory (2.4 Å,[56] 2.7 Å[41]).

To summarize this section, the contrast formation mechanism suggests that for obtaining morphological insight of the films care must be taken. As emphasized above, strongly polar tips can considerably influence the height representation in topography images, whereas neutral tips provide the right topography information. This aspect is of utmost importance when applying nc-AFM for MgO(001) thin films and is completely different to other thin film systems on conducting surfaces like alkali halide films on metal[36,37,40] or semiconducting substrates.[35,60] The reason for the special contrast formation of MgO islands results from the large dipole of the MgO film producing a positive net surface charge, which is considerably smaller for alkali halide films[41] and other insulating films supported on metal surfaces.

2.2 Work function measurements

In a second series of experiments, work function measurements were performed with a neutral tip[61] on a MgO film with a nominal coverage of roughly one monolayer. Such films are composed of mostly one- and occasionally two-layer-thick MgO islands,[20] as can be seen in the topography image a in Fig. 4 representing one and two layer thin islands with apparent heights of 2.2 Å and 4.4 Å, respectively, above the

silver surface (see profile b). Simultaneously to the acquisition of the topography image, a Kelvin image was obtained, which is shown in Fig. 4c. The MgO islands appear as dark islands in the Kelvin image, thus always showing a reduced work function of the silver substrate at the MgO islands. In characteristic regions where the silver surface can be seen (labeled with a bright dotted rectangle) and in regions of the one and two monolayer thin MgO islands (grey and dark grey dotted rectangles), histograms have been taken, which are shown in Fig. 4d. The three regions exhibit three distinctively different contact potentials with the tip. The difference between the values found for both types of islands and the value found for the silver surface yields the work function difference between silver and the MgO covered silver surface $\Delta\phi = (U_{CPD,MgO/Ag} - U_{CPD,Ag})e$. For both types of MgO islands, a mean value of $\Delta\phi_{1\text{–layer}} = (-1.1 \pm 0.2)$ eV and $\Delta\phi_{2\text{–layer}} = (-1.4 \pm 0.2)$ eV, respectively, could be found. These values are in good agreement with values calculated for one-layer- (−0.96 eV in this work, −0.71 eV,[13] −1.0 eV,[14] −0.94 eV[41]) and two-layer-thin films (−1.35 eV,[13] −1.2 eV,[14] −1.28 eV[41]).

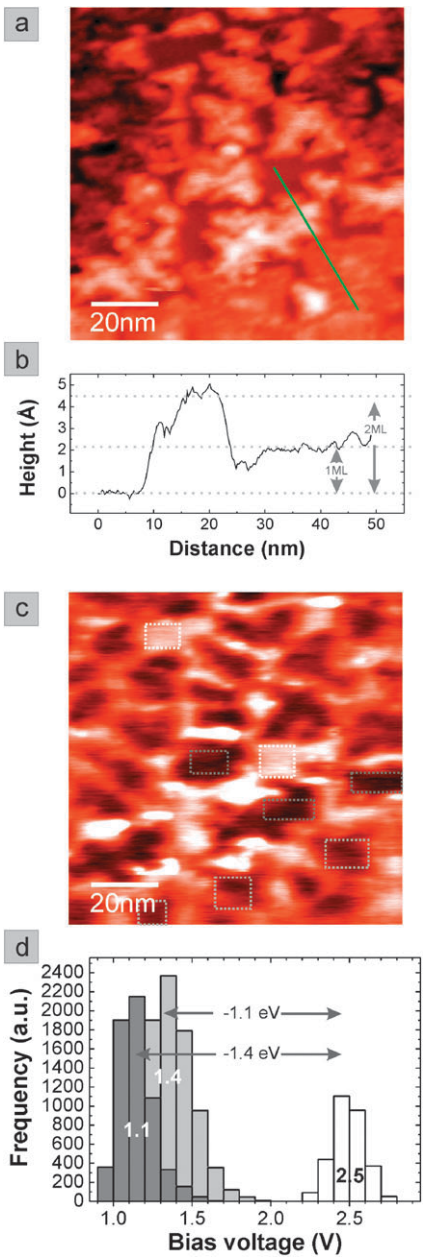

Fig. 4 Topography image (a) with representative profile (b) and corresponding Kelvin image (c) of one measurement obtained on a MgO film with a nominal thickness of 1 layer. The histogram in (d) shows the height distribution of those regions marked by the dotted squares. Bright rectangles mark regions of the silver substrate and grey, and dark grey rectangles mark 1 layer and 2 layer high MgO islands, respectively. The maxima of each height distribution corresponds to the contact potential between tip and each surface region. $100 \times 100\ nm^2$, $\Delta f = -71$ Hz, $v_{Scan} = 0.5$ Hz, $U_{ac} = 0.3$ V, $f_{ac} = 630$ Hz.

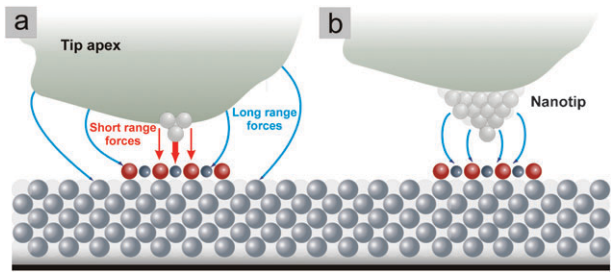

Fig. 5 (a) Interaction of the long-range electrostatic forces with the whole tip apex, which determines the contrast in KPFM. The short-range forces interact only with the last tip atoms/ions determining the contrast of topography images. (b) If the tip carries a nanotip, the lateral resolution is greatly enhanced in KPFM.

Other measurements (not shown) yielded also smaller work function differences, but larger values could not be observed. In KPFM it is well known that the electrostatic tip–surface interaction is of long-range character involving the complete tip apex into the contrast formation, whereas short-range forces are responsible for the topography contrast (Fig. 5a). The size of the tip apex therefore determines the lateral resolution, which is crucial for KPFM imaging of thin films.[36,37,60] If the islands are smaller than the tip apex, the tip apex integrates the electrostatic force not only above a MgO island, but also above the silver surface on the periphery of the MgO islands. Work function differences are then reproduced with smaller values, in agreement with EFS.[39] However, because the resolution depends on the tip size, it may happen that, *e.g.*, after tip changes so-called nanotips—microscopically small sub-tips at the blunt tip apex—are formed. These nanotips can strongly reduce the convolution effect of the blunt tip and therefore greatly increase the lateral resolution (Fig. 5b), which was obviously the case in the measurement shown in Fig. 4.

3. Conclusion

For the first time, the contrast formation in nc-AFM and KPFM of MgO(001) thin films supported on Ag(001) surfaces is elucidated. The topography contrast in nc-AFM images is mainly determined by the polarity of the tip. Especially polar tips strongly modify the topography contrast: the MgO islands are imaged as either dark or bright islands if the tip carries a polar group of cations or anions, respectively. However, for neutral, stoichiometric tips terminated by, *e.g.*, silver or stoichiometric MgO, the island topographies are correctly represented. Interestingly, these mechanisms in the contrast

formation are not observed for other ionic thin films like alkali halide thin films on conducting surfaces, which is due to the strong dipole of thin MgO(001) films.

Kelvin microscopy has been applied for the first time to extract work function differences between MgO islands and free regions of the silver substrate. As expected, the work function of silver is reduced by the MgO(001) thin islands and the values of 1 layer and 2 layer thin islands are in good agreement with values from theory.

Acknowledgements

This work was supported by the European COST program through Action D41 and by the European Science Foundation through the FANAS project NOMCIS. We acknowledge useful discussions with J. Goniakowski. U. H. also acknowledges support of the DFG and the HBFG. T. J. H. and A. S. F. acknowledges support from Academy of Finland *via* its Centre of Excellence programme and generous computer resources from the CSC, Helsinki, Finland. M. P. acknowledges support of the Alexander von Humboldt Foundation.

References

1 S. S. P. Parkin, C. Kaiser, A. Panchula, P. M. Rice, B. Hughes, M. Samant and S.-H. Yang, *Nat. Mater.*, 2004, **3**, 862–867.
2 S. Yuasa, T. Nagahama, A. Fukushima, Y. Suzuki and K. Ando, *Nat. Mater.*, 2004, **3**, 868–871.
3 K. McKenna, P. Sushko and A. Shluger, *J. Phys. Chem. C*, 2007, **111**, 2823–2826.
4 S. Giorgio, M. Cabie and C. R. Henry, *Gold Bull.*, 2008, **41**, 167–173.
5 C. Harding, V. Habibpour, S. Kunz, A. Farnbacher, U. Heiz, B. Yoon and U. Landman, *J. Am. Chem. Soc.*, 2009, **131**, 538–548.
6 R. Ferrando, G. Rossi, A. Levi, Z. Kuntová, F. Nita, A. Jelea, C. Mottet, G. Barcaro, A. Fortunelli and J. Goniakowski, *J. Chem. Phys.*, 2009, **130**, 174702.
7 J. Goniakowski, A. Jelea, C. Mottet, G. Barcaro, A. Fortunelli, Z. Kuntová, F. Nita, A. Levi, G. Rossi and R. Ferrando, *J. Chem. Phys.*, 2009, **130**, 174703.
8 A. Sanchez, S. Abbet, U. Heiz, W.-D. Schneider, H. Hakkinen, R. N. Barnett and U. Landman, *J. Phys. Chem. A*, 1999, **103**, 9573–9578.
9 B. Yoon, H. Häkkinen, U. Landman, A. S. Wörz, J.-M. Antonietti, S. Abbet, K. Judai and U. Heiz, *Science*, 2005, **307**, 403–407.
10 M. S. Chen and D. W. Goodman, *J. Phys.: Condens. Matter*, 2008, **20**, 264013.
11 C. R. Henry, *Surf. Sci. Rep.*, 1998, **31**, 231.
12 U. Heiz and U. Landman, *Nanocatalysis*, Springer Verlag, Berlin, 2007.
13 G. Butti, M. I. Trioni and H. Ishida, *Phys. Rev. B: Condens. Matter Mater. Phys.*, 2004, **70**, 195425.
14 L. Giordano, F. Cinquini and G. Pacchioni, *Phys. Rev. B: Condens. Matter Mater. Phys.*, 2005, **73**, 045414.
15 C. Zhang, B. Yoon and U. Landman, *J. Am. Chem. Soc.*, 2007, **129**, 2228.
16 M. Sterrer, T. Risse, M. Heyde, H.-P. Rust. and H.-J. Freund, *Phys. Rev. Lett.*, 2007, **98**, 206103.
17 D. Ricci, A. Bongiorno, G. Pacchioni and U. Landman, *Phys. Rev. Lett.*, 2006, **97**, 036106.
18 S. Schintke, S. Messerli, M. Pivetta, F. Patthey, L. Libioulle, M. Stengel, A. De Vita and W.-D. Schneider, *Phys. Rev. Lett.*, 2001, **87**, 276801.
19 S. Valeri, S. Altieri, U. Del Pennino, A. Di Bona, P. Luches and A. Rota, *Phys. Rev. B: Condens. Matter Mater. Phys.*, 2002, **65**, 245410.
20 S. Valeri, S. Altieri, A. Di Bona, P. Luches, C. Giovanardi and T. S. Moia, *Surf. Sci.*, 2002, **507–510**, 311–317.
21 S. Schintke and W.-D. Schneider, *J. Phys.: Condens. Matter*, 2004, **16**, R49–R81.
22 M. Sterrer, E. Fischbach, T. Risse and H. Freund, *Phys. Rev. Lett.*, 2005, **94**, 186101.
23 M. Sterrer, M. Heyde, M. Novicki, N. Nilius, T. Risse, H. Rust, G. Pacchioni and H. Freund, *J. Phys. Chem. B*, 2006, **110**, 46–49.
24 D. Ochs, W. Maus-Friedrichs, M. Brause, J. Günster, V. Kempter, V. Puchin, A. L. Shluger and L. N. Kantorovich, *Surf. Sci.*, 1996, **365**, 557–571.
25 S. Krischok, P. Stracke and V. Kempter, *Appl. Phys. A: Mater. Sci. Process.*, 2006, **82**, 167–173.
26 M. Vaida, T. Gleitsmann, R. Tchitnga and T. Bernhardt, *J. Phys. Chem. C*, 2009, **113**, 10264.
27 J. A. Farmer, N. Ruzycki, J. F. Zhu and C. T. Campbell, *Phys. Rev. B: Condens. Matter Mater. Phys.*, 2009, **80**, 035418.
28 S. Morita, R. Wiesendanger and E. Meyer, *Noncontact Atomic Force Microscopy*, Springer, Berlin, 2002.
29 F. Giessibl, *Rev. Mod. Phys.*, 2003, **75**, 949–983.
30 W. Hofer, A. Foster and A. Shluger, *Rev. Mod. Phys.*, 2003, **75**, 1287–1331.
31 D. A. Bonnell and J. Garra, *Rep. Prog. Phys.*, 2008, **71**, 044501.
32 C. Barth and C. R. Henry, *Phys. Rev. Lett.*, 2003, **91**, 196102.
33 S. Kitamura and M. Iwatsuki, *Appl. Phys. Lett.*, 1998, **72**, 3154–3156.
34 C. Barth and C. R. Henry, *J. Phys. Chem. C*, 2009, **113**, 247–253.
35 M. Goryl, F. Krok, J. J. Kolodziej, P. Piatkowski, B. Such and M. Szymonski, *Vacuum*, 2004, **74**, 223–227.
36 U. Zerweck, C. Loppacher, T. Otto, S. Grafström and L. Eng, *Phys. Rev. B: Condens. Matter Mater. Phys.*, 2005, **71**, 125424.
37 T. Glatzel, L. Zimmerli, S. Koch, B. Such, S. Kawai and E. Meyer, *Nanotechnology*, 2009, **20**, 264016.
38 M. Heyde, M. Sterrer, H. Rust and H.-J. Freund, *Appl. Phys. Lett.*, 2005, **87**, 083104.
39 T. König, G. H. Simon, H. Rust and M. Heyde, *J. Phys. Chem. C*, 2009, **113**, 11301–11305.
40 T. Filleter, W. Paul and R. Bennewitz, *Phys. Rev. B: Condens. Matter Mater. Phys.*, 2008, **77**, 035430.
41 S. Prada, U. Martinez and G. Pacchioni, *Phys. Rev. B: Condens. Matter Mater. Phys.*, 2008, **78**, 235423.
42 C. Barth and C. R. Henry, *Nanotechnology*, 2006, **17**, S155.
43 Although the voltage is physically applied to the tip, the electronics invert the voltage such that it appears as a voltage applied to the sample.
44 B. Terris, J. Stern, D. Rugar and H. Mamin, *Phys. Rev. Lett.*, 1989, **63**, 2669–2672.
45 R. M. Nyffenegger, R. M. Penner and R. Schierle, *Appl. Phys. Lett.*, 1997, **71**, 1878–1880.
46 http://gwyddion.net/, 2009.
47 G. Kresse and J. Furthmüller, *Comput. Mater. Sci.*, 1996, **6**, 15.
48 G. Kresse and J. Furthmüller, *Phys. Rev. B: Condens. Matter*, 1996, **54**, 11169.
49 J. P. Perdew, K. Burke and M. Ernzerhof, *Phys. Rev. Lett.*, 1996, **77**, 3865.
50 P. E. Blöchl, *Phys. Rev. B: Condens. Matter*, 1994, **50**, 17953.
51 G. Kresse and D. Joubert, *Phys. Rev. B: Condens. Matter Mater. Phys.*, 1999, **59**, 1758.
52 H. J. Monkhorst and J. D. Pack, *Phys. Rev. B: Solid State*, 1976, **13**, 5188.
53 R. Weast and C. R. Company, *CRC Handbook of Chemistry and Physics*, CRC Press Boca Raton, FL, 1988.
54 G. Geneste, J. Morillo and F. Finocchi, *Surf. Sci.*, 2003, **532–535**, 508–513.
55 J. Wollschläger, D. Erdös and K. M. Schröder, *Surf. Sci.*, 1998, **402–404**, 272–276.
56 A. Ferrari, S. Casassa and C. Pisani, *Phys. Rev. B: Condens. Matter Mater. Phys.*, 2005, **71**, 155404.
57 A. S. Foster, C. Barth, A. L. Shluger and M. Reichling, *Phys. Rev. Lett.*, 2001, **86**(11), 2373.
58 S. Morita and Y. Sugawara, *Thin Solid Films*, 2001, **393**, 310–318.
59 L. Nony, A. S. Foster, F. Bocquet and C. Loppacher, *Phys. Rev. Lett.*, 2009, **103**, 036802.
60 F. Krok, K. Sajewicz, J. Konior, M. Goryl, P. Piatkowski and M. Szymonski, *Phys. Rev. B: Condens. Matter Mater. Phys.*, 2008, **77**, 235427.
61 The tip was not used in UHV for a long time before the experiments shown in Fig. 4. Although charges at the tip apex do not flow off on a time-scale of the image acquisition, they decay, however, through the thin SiO_2 layer into the conducting body of the doped silicon tip on a time-scale of hours and days.[58] Therefore, it can be strongly anticipated that the tip used for the experiments was indeed a 'neutral tip'.
62 P. V. Sushko, J. L. Gavartin and A. L. Schluger, *J. Phys. Chem. B*, 2002, **106**, 2269.